

# Testing the fracture of spectacle lenses

Stephen K. Lucas<sup>1</sup> and James M. Hill<sup>2</sup>

## Abstract

SOLA International is a company based in Adelaide which produces a wide range of optical lenses, including those for spectacles and over 100 million of their product are being worn around the world today. Impact performance of lenses is a critical safety requirement, and yet the problem of fracture of lenses by impact of a ball bearing is not properly understood. However, it is known that both thinness and flatness tend to reduce impact strength, while lens coating facilitates the fracture process, and tends to focus the fracture load regime. Generally, crack initiation and propagation is a complex and not well understood issue. Ideally, SOLA International seeks a mathematical model which inputs lens geometry and material properties and is able to predict the deformation on impact. In particular, prediction of the stresses in the back surface coating is important. The mathematical model might then provide an alternative framework to laboratory tests, which are labourious and frequently not reproducible. The full solution of this problem involves many physical processes, including impact phenomenon, the relationship of static test results to impact tests, contact mechanics, random effects appearing through flaws and microcracks, fracture mechanics and finally crack propagation. In addition, the full problem in reality involves dynamic deformations of a visco-elastic body, coated with material of different physical properties, and it is required to formulate conditions under which crack initiation will take place. A modest attempt towards some of these issues is outlined below.

## 1 Introduction

### 1.1 The Company SOLA International

SOLA began in 1956, with nine optical technicians experimenting in a garage in Adelaide. Their goal was to cast spectacle lenses from recently discovered plastic materials. After a few early successes, those pioneers founded SOLA ( Scientific Optical Laboratories of Australia) in 1960. SOLA's first overseas subsidiary opened in Japan, in 1968, and in ensuing years, operations were added throughout Asia, Europe and the Americas. In 1979, SOLA was acquired by Pilkington plc, and in 1988 the corporate headquarters moved from Adelaide to Menlo Park, California. The company's global expansion continued during the

---

<sup>1</sup>Centre for Industrial and Applicable Mathematics, School of Mathematics, University of South Australia, Mawson Lakes SA, 5095. email [S.Lucas@unisa.edu.au](mailto:S.Lucas@unisa.edu.au)

<sup>2</sup>School of Mathematics and Statistics, University of Wollongong, Wollongong NSW, 2522. email [jim\\_hill@uow.edu.au](mailto:jim_hill@uow.edu.au)

1980's, with new manufacturing operations opening in Venezuela, Taiwan and China. In 1993, SOLA was purchased by AEA Investors Inc., and in March 1995 the company was listed on the New York Stock Exchange. Further growth came from new products, international expansion and through the acquisitions of US lensmakers Neolens and American Optical.

SOLA's regional structure now includes North America, Europe, Asia, Australia, South America and an international Sunlens Division. Across the world over 100 million people wear SOLA lenses. The company now operates major research and development centres in Adelaide and Petaluma, California; supported by a specialist process engineering team at a plant in Wexford, Ireland. From SOLA's earliest years, lens technology has continued to evolve. The result is thinner, lighter lens forms, innovative new designs and high performance coatings to achieve optical excellence.

## 1.2 The Problem

To satisfy FDA safety requirements for sale in the USA, all spectacle lenses must comply with the "drop-ball impact test". This test simply involves dropping a steel ball of diameter 15.9 mm weighing 16.36 g onto the outer surface of the lens from a height of 1.27 m. The lens is held in place on a silicon ring on a supporting plate, with an additional load ring placed above to keep it in position. The steel ball can be guided, and must impact the lens near its center. The central region of the lens deflects as the ball strikes, and cracks may form, which could lead to the fracture of the lens. The lens passes the test if it doesn't break. There is a similar European ISO/CEN test for spectacle lenses, which involves a "static load", rather than an impact. In this case a force of 100 Newtons is applied to the outer surface of the lens, through a steel ball. The load is applied for 10 seconds, and then removed. The lens passes if it does not break, or deform too far on its center line.

There are several factors that could contribute to whether a lens passes the above tests.

- *Nature of the lens material.* The material properties of the lens determine how it will deform under a load, and can also affect the way in which cracks propagate through the material. Chemical treatments to the lens surface could modify its susceptibility to cracks forming and propagating.
- *Coatings to the back surface.* Most lenses are coated with a hard glassy material to enhance scratch resistance, or to produce modified optical characteristics, such as reduced glare. These coatings are often much more brittle than the bulk lens material, and cause the lens to break at much lower forces than when uncoated. However, these layers are typically only a few microns thick, and so will not have a significant effect on the overall deformation of the lens (which is of the order of 2 mm thick at the center).

- *Lens power and curvature.* Minus powered lenses are the ones in which impact problems are most likely to occur. In these lenses, the radius of curvature of the front of the lens is larger than the back, leading to lenses which are thinnest at the center. For a given lens power and front curvature, there is a simple relationship between the thickness of the lens at the center and the curvature of the back surface. The perennial search for thinner lighter lenses lead to choosing the flattest possible curves and the thinnest possible centers, both of which will make the lens more likely to fail an impact test.

There are a number of issues of interest to SOLA. The first and most useful result would be a model for the deformation and stress within of a lens, under both the impact and static tests, based on the lens form and material properties. This could then be used to model the deformation and stresses within the back surface coating, which would lead to an analysis of crack initiation and/or propagation. A full solution to this problem turned out to be well beyond the capacity of the MISG study group. However, some initial results are presented below.

## 2 Geometry

The power of a lens  $P$  is defined as the inverse of its focal length, which is the distance from the lens at which rays initially parallel are bent to go through the same point, called the focus. The power is usually measured in dioptres ( $D$ ), where  $P = 530/r$  with  $r$  being the radius of curvature measured in mm. For a negative power lens, the focus is a virtual point (see Figure 1) and the focal length is negative. In practical lens design, a negative power lens is usually formed as in Figure 1(c), where both front and back curves have positive power. For this lens form the thinnest part of the lens is at its center, the point of impact in the tests, and so negative power lenses are most likely to cause problems under impact. In the case of 1(c), Stephenson [17] gives the relationship between lens center thickness  $t$ , front surface curvature  $r_f$ , back surface curvature  $r_b$  (all in mm), refractive index of the lens material  $n$  and lens power  $R_x$  (in  $D$ ) as

$$\frac{1}{r_b} = \frac{1}{r_f - t \left(\frac{n-1}{n}\right)} - \frac{R_x}{(n-1)10^3}. \quad (1)$$

Practically,  $r_f$  varies between 117.8 mm and 176.7 mm,  $t$  lies between 1.5 mm and 2.5 mm, the lens diameter lies between 70mm and 81.75 mm.

We include here two sets of results for the material CR-39, which has a refractive index  $n = 1.499$ . In Figure 2(a), we choose  $r_f = 121.8$ ,  $t = 1.5, 2.0, 2.5$ , and plot  $r_b$  versus  $R_x$ , showing how varying the back surface can alter the power of the lens. It is immediately obvious that the surface thickness has a very small effect on the lens power – a variation of about 0.02 between the three curves.

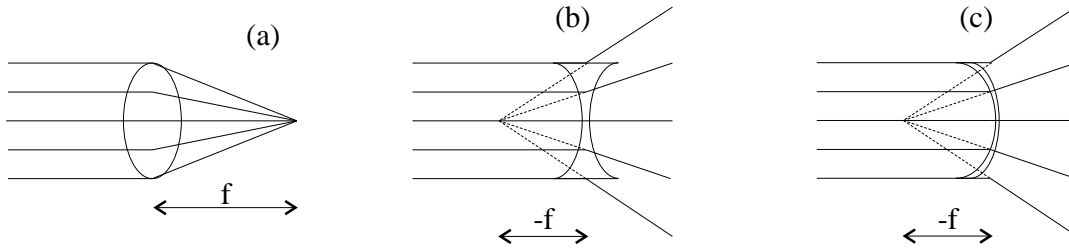


Figure 1: Focal length  $f$  for (a) positive and (b) negative power lenses

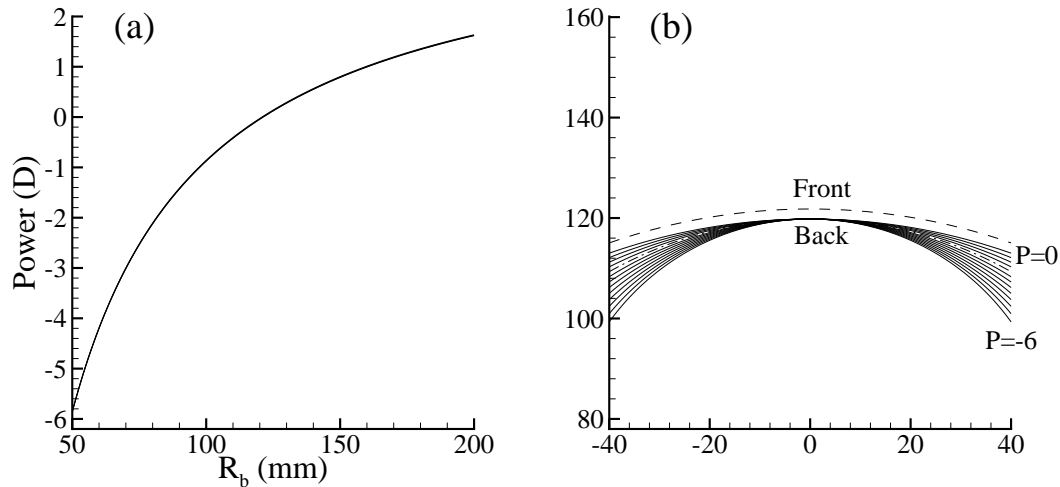


Figure 2: Using data from text, (a) radius of curvature of back lens versus lens power, and (b) lens geometry for various powers.

Figure 2(b) chooses  $r_f = 121.8$ ,  $t = 2.0$ ,  $R_x = 0, -0.5, \dots, -6.0$ , and instead of simply calculating  $r_b$  (the inverse of Figure 2(a)), shows the actual back lens position (with a diameter of 80mm). The front lens position is included as a dashed line, and the power -2 back lens is the dot-dash line. We see that the power 0 lens is almost equal thickness, but increasing the power leads to an increasingly large lens edge. Choosing  $t$  smaller would reduce the thickness of the edge, but cause problems with passing the impact tests. SOLA indicated that the -2 power lens was the most prone to failing impact testing, but they do not usually make lenses of smaller negative power, so the lenses with thicker edges are less likely to fail. We will discuss this further in a later section.

One last minor point is that lenses surfaces are not usually exactly spherical in shape. These variations are well defined, and are very small in size compared to the spherical approximation. Here, we will continue to assume the lens surfaces are spherical.

### 3 Static or Dynamic?

The FDA impact test is obviously dynamic, with the force from the dropping ball being applied for a relatively short period of time (of the order of 2 milliseconds according to SOLA). The ISO/CEN test is static, in that the load is slowly applied, then kept constant. Obvious questions are whether these tests are comparable, and whether the dynamic test can be considered as quasistatic, where the problem can be solved as if it is static in terms of an instantaneous applied load, and a collection of static solutions be solved at various instants in time. The text by Goldsmith [6] is an excellent starting point for studying impact problems.

#### 3.1 Test Equivalence

The static test involves a load of 100 Newtons, while the dynamic test involves dropping a steel ball weighing 16.36 grams from a height of 1.27 meters. Consider the following very simplified estimate, based on the high school physics formula  $v^2 = u^2 + 2as$ , where  $v$  is final velocity,  $u$  is initial velocity,  $a$  is (constant) acceleration, and  $s$  is displacement. A ball falling 1.27 meters from rest will have a final velocity of  $\sqrt{24.892}$ . Assuming that the ball decelerates to rest in 2 mm, the acceleration becomes 6223 meters per second squared. The equivalent force from  $F = ma$  becomes 101.8 Newtons – remarkably close to the static result! More typical deflections of the lens are of the order of 1.5 mm, which leads to a force of 136 Newtons. This is still remarkably close. However, experience shows that a lens which passes the static test can fail the dynamic test.

What is needed at this point is a more careful look at the experimental data for a particular lens, specifically what force is required to break the lens during the static test, and then what force (and deflection) is observed for the dynamic test in a case where the lens “just” breaks. It may be that the size of the actual forces leading to fracture of the lens is in fact the same, and that the dynamic test is actually more rigorous than the static test.

#### 3.2 Wave speeds

One way of deciding the importance of dynamic effects is to look at the time scales of how long various waves take to travel through an elastic medium. There are two forms of waves (see eg Timoshenko & Goodier [20]): longitudinal and transverse. Longitudinal (particles move parallel to wave direction) waves, with wave speed  $c_l$  and transverse (particles move perpendicular to wave direction)

waves with wave speed  $c_t$  satisfy

$$c_l = \sqrt{\frac{E(1-\nu)}{(1+\nu)(1-2\nu)\rho}}, \quad c_t = c_l \sqrt{\frac{1-2\nu}{2(1-\nu)}}. \quad (2)$$

For the material CR-39, with  $E = 2.07 \times 10^9$  Pa,  $\nu = 0.4$ , and  $\rho = 1310$ , we have that  $c_l = 1840$  and  $c_t = 751$ . The time for waves to travel across the thickness of a lens (say 2 mm) are  $1.1 \times 10^{-6}$  and  $2.7 \times 10^{-6}$  seconds respectively. Considering the fact that experimentally the impact takes of the order of  $2 \times 10^{-3}$  seconds, we could assume that this is indeed a quasistatic situation.

However, it was suggested that a more important time scale is that for bending waves to travel through the body. This time scale is of order  $l^2 \sqrt{h\rho/D}$ , where  $l$  is the length of the body involved,  $h$  its width, and  $D$  the plate bending stiffness (see later). For CR-39 with  $l = 0.04$ , we find the time scale is  $2 \times 10^{-3}$  seconds, comparable with the time of impact.

After further consideration, we now believe that this time scale is not relevant to the problem of whether the dynamic lens problem can be considered as a quasistatic one. The bending wave time scale indicates a time scale for how long the entire lens takes to bend due to impact, then return to its initial shape. It is quite reasonable for this time to be similar to the time of contact between the ball and lens. It appears that the lens impact problem can be solved as a quasistatic one. However, a more convincing argument would be to consider the simpler problem of the dynamic response of a beam to an applied force.

## 4 Layers of Cylindrical Shells

The full solution to the deformation of an elastic solid under a prescribed combination of deformations and applied forces also depends on the geometry and elastic properties of the solid. One of the most important assumptions in the theory of linear elasticity is that deformations (strains) are directly proportional to forces (stresses). While this leads to a linear set of partial differential equations, most practical problems cannot be solved by analytic means (see for example Timoshenko & Goodier [20], Barber [2] and Landau & Lifshitz [9]) and require numerical methods, such as finite element (e.g. Kikuchi [8]) or boundary element (e.g. Brebbia *et al.* [3]) methods. Note that both [3] and [8] include discussion of numerical methods for plates.

Most elasticity theory is based upon knowledge of either the imposed deformation or applied force at every point on the boundary of the elastic solid. A more difficult class of problems are the so-called contact problems, where two elastic bodies are in contact with each other. A variety of methods can be used to formulate these problems. More details can be found in, for example, Johnson [7], Gladwell [5], and Zhong [23].

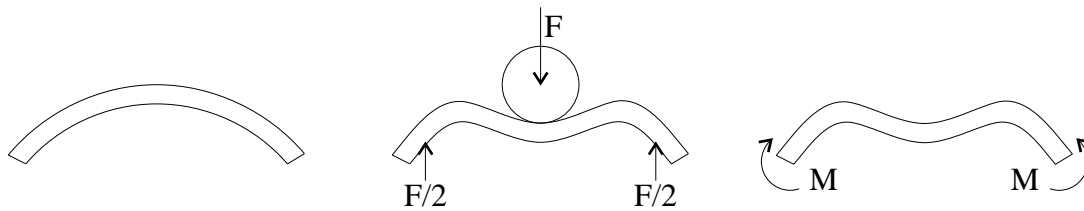


Figure 3: For a cylindrical shell, (a) a slice of the undeformed shell, (b) deformed by a line load, simply supported at the edges, and (c) the equivalent moment problem.

A spectacle lens is essentially a shallow spherical shell, formed from a thin shell of spherical shape, and sliced off using a horizontal cut. Spectacle lenses are not normally of constant thickness throughout, although low power lenses are close to constant thickness to a first approximation. While there are no analytic solutions for spherical shells known to the authors, there are solutions available for cylindrical shells. Although this analysis will not give the “right” answers, it will give a useful guide to what we expect to happen in the spherical case. Consider an infinitely long cylindrical shell of constant thickness, a slice of which is shown in Figure 3(a), with coordinates  $r$ ,  $\theta$  in the plane and  $z$  into the figure. The deformation of the cylindrical shell is caused by an infinitely long line force, acting as shown in Figure 3(b), which is equivalent to the problem of a cylindrical shell deformed by a moment of magnitude  $M$ , as shown in Figure 3(c).

The solution to the moment problem in Figure 3(c) is (for example, Barber [2])

$$\begin{aligned}
 u_\theta &= \frac{4Br\theta}{E}, & u_r &= \frac{1}{E} \left[ -\frac{(1+\nu)(A+Br^2)}{r} + 2(1-\nu)r(B \ln r + C) \right], \\
 \sigma_{rr} &= \frac{A}{r^2} + B(1+2 \ln r) + 2C, & \sigma_{\theta\theta} &= -\frac{A}{r^2} + B(3+2 \ln r) + 2C,
 \end{aligned} \tag{3}$$

where  $u_r$ ,  $u_\theta$  are the deformations in the radial and angular directions,  $\sigma_{rr}$ ,  $\sigma_{\theta\theta}$  are stresses, and  $E$  is Young’s modulus and  $\nu$  is Poisson’s ratio for the material. The constants  $A$ ,  $B$  and  $C$  are to be found from the boundary conditions of zero stress on the inner and outer surfaces of the lens. In terms of the constants  $A$ ,  $B$  and  $C$  the moment  $M$  is given by  $M = A \ln(b/a) + B(b^2 \ln b - a^2 \ln a) + C(b^2 - a^2)$ , where the inner and outer edges of the shell are at positions  $r = a$  and  $r = b$  respectively.

If we now suppose that the actual lens occupies the region  $(b, c)$  and is subscripted by the numeral 2, while the regions  $(a, b)$  and  $(c, d)$  constitute extremely thin inner and outer layers subscripted by 1 and 3 respectively, then the conditions of zero stress on the inner and outer surfaces and the continuity of displacements and radial stress  $\sigma_{rr}$  at the interfaces yields the following

boundary conditions:

$$\begin{aligned}
\sigma_{rr1}(a) &= 0, \\
\sigma_{rr1}(b) &= \sigma_{rr2}(b), \quad u_{r1}(b) = u_{r2}(b), \quad u_{\theta1}(b) = u_{\theta2}(b), \\
\sigma_{rr2}(c) &= \sigma_{rr3}(c), \quad u_{r2}(c) = u_{r3}(c), \quad u_{\theta2}(c) = u_{\theta3}(c), \\
\sigma_{rr3}(d) &= 0,
\end{aligned} \tag{4}$$

and from these relations we may ultimately deduce the following expression for the applied moment  $M$ :

$$\begin{aligned}
M &= A_1 \ln(b/a) + B_1(b^2 \ln(b) - a^2 \ln(a)) + C_1(b^2 - a^2) + A_2 \ln(c/b) \\
&+ B_2(c^2 \ln(c) - b^2 \ln(b)) + C_2(c^2 - b^2) + A_3 \ln(d/c) \\
&+ B_3(d^2 \ln(d) - c^2 \ln(c)) + C_3(d^2 - c^2).
\end{aligned} \tag{5}$$

On using the following values of the material constants and the radii  $a, b, c$  and  $d$ , Figure 4 shows the variation with the applied moment  $M$  in the hoop stress  $\sigma_{\theta\theta}$ , evaluated at the inner surface  $r = a$ .

$$\begin{aligned}
\nu_1 &= 0.3, \quad \nu_2 = 0.4, \quad \nu_3 = 0.3, \\
E_1 &= 0.70 \times 10^{11}, \quad E_2 = 0.2 \times 10^{10}, \quad E_3 = 0.70 \times 10^{11}, \\
a &= 0.120, \quad b = 0.120003, \quad c = 0.122003, \quad d = 0.122006.
\end{aligned} \tag{6}$$

The typical numbers produced by equation (5) are consistent with SOLA's experience and therefore this result represents a mechanism to arrive at rough estimates of the hoop stress at the inner or back surface layer of the lens.

## 5 Plates and Shells

While there is an extensive literature on problems involving plates and shells, and many excellent texts (eg Timoshenko & Woinowsky-Krieger [19] and Szilard [18]), we could find relatively little of use to us on contact or obstacle problems. A closely related solution can be found in Essenburg [4], where the solution for the deformation of a clamped circular plate by a paraboloid of revolution is derived. However, the classical plate equations are adjusted to allow for transverse shear deformation, and while the paper indicates that far better results are obtained than those using classical theory, it is beyond the scope of our interest. Westbrook [21] reformulates obstacle problems for beams and plates as variational inequalities, and solves them using finite elements. While classical theory is used, the problem addressed is one where the beam or plate is deformed by a given force, with a rigid barrier that may impede its deformation. We are more interested in the case where the applied force is not known a priori, but comes out as a function of the position of the indenting sphere. Finally, Yau & Gao [22] in a sense extend Westbrook's work (although completely independently)

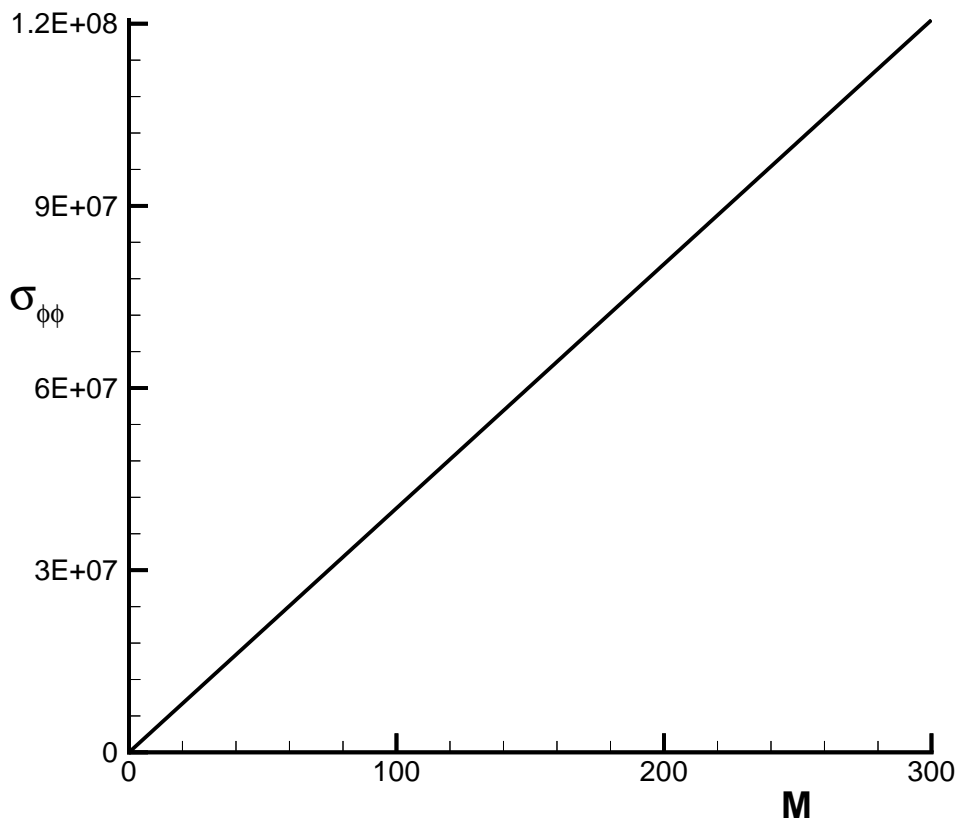


Figure 4: Variation of the hoop stress at  $r = a$  with respect to moment.

by developing a nonlinear variational inequality for the obstacle problem using the von Kármán equations (thin plates with deformations large compared to the plate thickness). They discuss uniqueness and existence of solutions, but do not develop numerical techniques based on their results.

## 5.1 Classical Plate Theory

A plate is a flat noncurved solid whose thickness is small compared with its other dimensions (at least an order of magnitude smaller than its smallest lateral dimension). Its middle surface is defined as a surface that bisects the plate in its thickness dimension. We assume that the material of the plate is elastic, homogeneous and isotropic, the plate is of equal thickness throughout, and that deflections are small compared to plate thickness (typically up to 1/5 of the thickness). We also assume that the slopes of the deformed middle surface are small, that straight lines initially normal to the middle surface remain straight and normal to the middle surface (ie transverse shear is neglected), that stresses normal to the middle surface are negligible, and that the deflection of the plate is produced by the displacement of points of the middle surface normal to its initial surface.

Under these conditions, the classical equations of elasticity can be used to derive the governing differential equation of a plate subjected to lateral loads (see, for example [18, §1.2], whom we follow in the discussion of this section) as

$$D\nabla^2\nabla^2w = p_z, \quad (7)$$

where  $w$  is the deflection of the plate under the lateral load  $p_z$ , and  $\nabla^2$  is the Laplacian operator. It is usual to assume that the initially flat plate's middle surface lies in the  $x$ - $y$  plane, and deflection is positive in the negative  $z$  direction. The constant  $D = Eh^3/12(1 - \nu^2)$  is known as the flexural rigidity of the plate, with  $E$  its Young's modulus,  $\nu$  its Poisson's ratio, and  $h$  its thickness. Equation (7) is a fourth order nonhomogeneous partial differential equation whose solution can often be found analytically. The bending moments acting on the plate can be found in terms of  $w$  as

$$m_x = -D \left( \frac{\partial^2 w}{\partial x^2} + \nu \frac{\partial^2 w}{\partial y^2} \right), \quad m_y = -D \left( \frac{\partial^2 w}{\partial y^2} + \nu \frac{\partial^2 w}{\partial x^2} \right). \quad (8)$$

For a circular plate with axisymmetric loading and boundary conditions,  $w$  is independent of  $\theta$ , and (7) can be rewritten as the ordinary differential equation, with the Laplacian operator  $\nabla_r^2 = \frac{d^2}{dr^2} + \frac{1}{r} \frac{d}{dr}$ ,

$$\nabla_r^2 \nabla_r^2 w(r) = \frac{d^4 w}{dr^4} + \frac{2}{r} \frac{d^3 w}{dr^3} - \frac{1}{r^2} \frac{d^2 w}{dr^2} + \frac{1}{r^3} \frac{dw}{dr} = \frac{p_z(r)}{D}. \quad (9)$$

The bending moments in this case are

$$m_r = -D \left( \frac{d^2 w}{dr^2} + \frac{\nu}{r} \frac{dw}{dr} \right), \quad m_\theta = -D \left( \nu \frac{d^2 w}{dr^2} + \frac{1}{r} \frac{dw}{dr} \right). \quad (10)$$

A variety of physically realistic boundary conditions are available for plate problems. The one we will be interested in pursuing here for circular plates is the simple support,

$$w(r)|_{r=r_0} = 0, \quad m_r(r)|_{r=r_0} = -D \left( \frac{d^2 w}{dr^2} + \frac{\nu}{r} \frac{dw}{dr} \right) \Big|_{r=r_0} = 0, \quad (11)$$

which is equivalent to the plate sitting on a rigid support at radius  $r_0$  with deflection and bending moment zero.

The governing equation (9) with boundary conditions (11) can be easily solved analytically for a particular load  $p_z$ . Using linearity, the solution can be written as the sum of homogeneous ( $w_h$ ) and particular ( $w_p$ ) solutions. The solution to the homogeneous ode  $\nabla_r^2 \nabla_r^2 w_h = 0$  can be written as  $w_h = C_1 + C_2(r/r_0)^2 + C_3 \ln(r/r_0) + C_4 r^2 \ln(r/r_0)$ . For the deflections and moments at the center of the plate to be well behaved, we require  $C_3 = C_4 = 0$  (for the case of an annular plate, these constants would be set by adding additional boundary conditions at the inner edge of the annulus). The particular solution  $w_p$  can be found by direct integration of (9) as

$$w_p(r) = \frac{1}{D} \int_0^r \frac{1}{\delta} \left\{ \int_0^\delta \gamma \left[ \int_0^\gamma \frac{1}{\beta} \left( \int_0^\beta p_z(\alpha) \alpha d\alpha \right) d\beta \right] d\gamma \right\} d\delta. \quad (12)$$

In the case of  $p_z(r)$  being either a point load at the center of the plate, or a ring load at some radius  $a$ , the deflections can be found in similar ways, with the discontinuities in the third derivative depending on the total load, and the boundary conditions giving the value of the constants. For a point load of strength  $P$  at the center of the plate with simple support, the deflection is

$$w(r) = \frac{Pr_0^2}{16\pi D} \left[ \frac{3 + \nu}{1 + \nu} \left( 1 - \frac{r^2}{r_0^2} \right) + 2\rho^2 \ln \frac{r}{r_0} \right]. \quad (13)$$

For a ring load of total load  $P$  at radius  $r_1$ , the deflection with simple support is

$$w(r) = \begin{cases} \frac{P}{8\pi D} \left[ (r_1^2 + r^2) \ln \frac{r_1}{r_0} + (r_0^2 - r_1^2) \frac{(3 + \nu)r_0^2 - (1 - \nu)r^2}{2(1 + \nu)r_0^2} \right], & r \leq r_1, \\ \frac{P}{8\pi D} \left[ (r_1^2 + r^2) \ln \frac{r}{r_0} + (r_0^2 - r^2) \frac{(3 + \nu)r_0^2 - (1 - \nu)r_1^2}{2(1 + \nu)r_0^2} \right], & r \geq r_1. \end{cases} \quad (14)$$

## 5.2 Spherically Prescribed Deflection

We are interested in finding the deformed shape of a circular plate due to contact with a rigid sphere at a given height, and also finding the required load  $p_z$ , since

$2\pi \int_0^{r_0} p_z(r)r dr$  is the total force with which the sphere pushes on the plate. The technique we anticipate using is common to many contact problems. Assume a certain proportion of the sphere is in contact with the plate. In the contact region, the deformation is the shape of the sphere. There is no load on the rest of the plate, and so a solution can be found which takes into account the edge boundary conditions. We then require continuity of the deformation and its first and second derivatives at the point where the sphere leaves the plate. These conditions cannot in general be satisfied, and in principle we end up with a single nonlinear equation for the proportion of the sphere that contacts the plate. Once this has been found to satisfy continuity,  $p_z$  and the total load on the plate can be calculated. For a much more general discussion on contact-impact problems and contact regions within the domain of finite element approximation methods, see Zhong [23] and Gladwell [5].

Assume that the undeformed plate is in the  $x$ - $y$  plane, and the deformation  $w$  is measured as positive in the negative  $z$  direction. The plate is deformed by a sphere of radius  $R$  and center  $(x, y, z) = (0, 0, c)$  (we require  $R - c > 0$  so that the sphere actually contacts the plate). If  $r_1$  is the radius of the region of contact between the plate and the sphere, then the deformation of the plate is  $w(r) = -c + \sqrt{R^2 - r^2}$  for  $0 \leq r \leq r_1$ . Note that the geometry requires  $r_1 < R$ , and the minus sign in front of the  $c$  is due to  $w$  begin positive down. Then, on  $[0, r_1]$  from (9), the load due to the spherical deformation is

$$\frac{p_z(r)}{D} = \frac{-8R^4 - 8R^2r^2 + r^4}{(R^2 - r^2)^{7/2}}. \quad (15)$$

An immediate problem is that  $p_z(0) = -8/R^3 < 0$ . The real positive solution to  $r^4 - 8R^2r^2 - 8R^4 = 0$  is  $r = \sqrt{4 + 2\sqrt{6}}R$ , which is greater than  $R$ , and so  $p_z(r) < 0$  on  $[0, r_1]$ . This indicates that to force the inner part of the plate to take the shape of a sphere, a force is required to push the plate up onto the sphere. This is clearly not a physically reasonable result, and so the plate cannot take the shape of a sphere on any finite region  $[0, r_1]$  due to contact alone. This indicates that perhaps a point load solution is more appropriate as a solution to this contact problem.

### 5.2.1 Point Source Solution

The solution in (13) above is the deformation of a thin circular plate with a point load at its center, with simply supported edges. We are interested in whether these solutions can be matched with the deformation due to contact with the sphere. If the sphere only touches the plate at  $r = 0$ , then we have that

$$P = \frac{16\pi D(R - c)(1 + \nu)}{r_0^2(3 + \nu)}. \quad (16)$$

The deformation due to this point load is then

$$w(r) = (R - c) \left[ 1 - \rho^2 + \frac{1 + \nu}{3 + \nu} 2\rho^2 \ln \rho \right]. \quad (17)$$

Unfortunately, this solution is not acceptable. For a finite length the surface of the sphere is below that of the plate, a physically impossible situation. We can see this by considering the radius of curvature of the solution (17). Using the fact that the radius of curvature of the function  $y = f(x)$  is  $\sqrt{1 + (f'(x))^2} / f''(x)$  (with a negative solution indicating the center of the circle is down), derivatives of the solution in (17) shows that the curve has radius of curvature zero at  $r = 0$ . Since the sphere has radius of curvature  $R$ , near  $r = 0$  the curve for the plate is above that of the sphere.

### 5.2.2 Ring Source Solution

Johnson [7] is a classic text on contact problems, and includes a two page section on plates and shells. The example considered in most detail is a flat plate of length  $2l$ , width  $w$  and thickness  $2b$  deformed by contact with a rigid cylinder of radius  $R$  whose axis is perpendicular to the length of the plate, such that the contact arc is  $2a$  (as in figure 3(b) earlier). Johnson then states that the contact loading is along two lines parallel to the axis of the cylinder at positions  $x = \pm a$ , and with a given load  $P$  the position of the contact  $a$  satisfies  $P(l - a)/2 = 2Ewb^3/3R(1 - \nu^2)$ . Without any more detail, Johnson observes that as the load increases, the pressure is concentrated at the edges. He also mentions, with reference to Essenburg [4], that the contact pressure due to a circle of contact is concentrated into a ring of force, which we will now investigate.

The deformation of a circular plate by a ring force at radius  $r_1$  with force per unit length  $p$  and total load  $P = 2\pi r_1 p$  with simple support is given by (14). After extensive algebra, one can show that these solutions are the same as using the approach that the plate is deformed a specific distance at  $r = r_1$ , with no other load and continuity of deformation and its first derivative across  $r = r_1$ . We find that the second derivative of the deformation is continuous, and there is a discontinuity in the third derivative of magnitude  $P/2\pi D r_1 = p/D$ , the force per unit length of the ring force scaled by  $D$ . This result is encouraging, since we would expect a discontinuity in the third derivative of the solution of a fourth order equation with a point force.

Given that the deformation is caused by a sphere with center a distance  $c$  above the undeformed plate position, we wish to find the point  $r_1$  and load  $P$  such that the ring source solution touches the sphere at  $r = r_1$  with tangent the same as that of the sphere. For the simply supported case, we find from (14)

and its derivative that we require

$$\left. \begin{aligned} \frac{P}{8\pi D} \left[ 2r_1^2 \ln \frac{r_1}{r_0} + (r_0^2 - r_1^2) \frac{(3 + \nu)r_0^2 - (1 - \nu)r_1^2}{2(1 + \nu)r_0^2} \right] &= -c + \sqrt{R^2 - r_1^2}, \\ \frac{P}{8\pi D} \left[ 2r_1 \ln \frac{r_1}{r_0} - (r_0^2 - r_1^2) \frac{(1 - \nu)r_1}{(1 + \nu)r_0^2} \right] &= \frac{-r_1}{\sqrt{R^2 - r_1^2}}. \end{aligned} \right\} \quad (18)$$

These can be rewritten as

$$P = \frac{8\pi D}{\sqrt{R^2 - r_1^2}} \left/ \left[ \left( 1 - \frac{r_1^2}{r_0^2} \right) \frac{(1 - \nu)}{(1 + \nu)} - \ln \frac{r_1}{r_0} \right] \right., \quad (19)$$

and

$$\frac{\left[ 2r_1^2 \ln \frac{r_1}{r_0} + (r_0^2 - r_1^2) \frac{(3 + \nu)r_0^2 - (1 - \nu)r_1^2}{2(1 + \nu)r_0^2} \right]}{\sqrt{R^2 - r_1^2} \left[ \left( 1 - \frac{r_1^2}{r_0^2} \right) \frac{(1 - \nu)}{(1 + \nu)} - \ln \frac{r_1}{r_0} \right]} = -c + \sqrt{R^2 - r_1^2}. \quad (20)$$

For any given problem, one could specify  $r_0$ ,  $\nu$ ,  $R$ ,  $D$ , then given any  $c$ , solve (20) for the position of the ring load  $r_1$ , then substitute in (19) to explicitly find the total load. However, the approach we will take here is to choose various  $r_1$ , and see how  $c$  changes by solving (20) explicitly.

For a particular test lens, we choose  $r_0 = 3.5 \times 10^{-2}$ ,  $\nu = 0.4$ ,  $R = 7.95 \times 10^{-3}$  (lengths in meters), and are interested in varying  $r_1$  so that  $c$  lies in the range of  $7.95 \times 10^{-3}$  down to  $5.95 \times 10^{-3}$ , which corresponds to a deformation of the plate of zero up to two millimeters. Figure 5 shows the results with these parameter values, where we found the limits of  $r_1$  by trial and error. Noting in particular the logarithmic scale, we see that the position of the radius is at most  $10^{-40}$  meters – about 24 orders of magnitude smaller than the nucleus of an atom. This is so incredibly small that it is beyond the limit at which the continuum hypothesis can be applied for an elastic solid. This tells us that despite the results of section 5.2.1 above, the contact between a rigid sphere and a thin plate, at least in the small deformation case, is a single point, so the loads and deformations in (16) and (17) respectively are the ones we should use.

### 5.3 Additional Formulations

During the period of the MISG meeting, several other useful formulations were found for plates and shells that would be appropriate to this project. While no one of them individually will give a solution to the full lens problem, they each address one of the issues in the full problem.

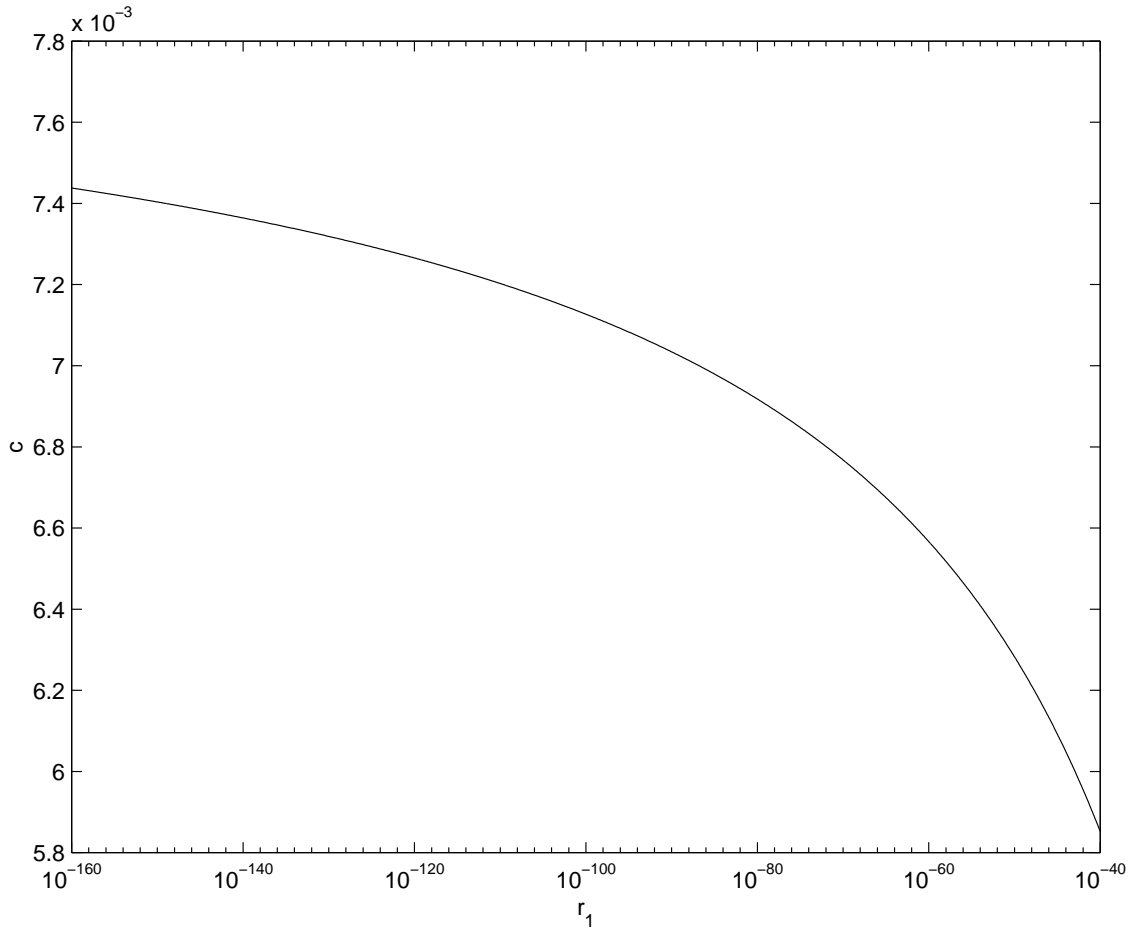


Figure 5: Sphere center  $c$  versus radius of ring load  $r_1$ .

### 5.3.1 Plates with Large Deformations

The work described previously on plates is considered valid for the deflection of the plate being small in comparison to the thickness of the plate. In the regime where linear elastic theory is still applicable, but the deformation is of the same order or larger than the plate thickness, the theory needs to be adjusted. Lateral deflections of the middle surface of the plate are now accompanied by stretching, which can substantially increase the plate's load-carrying capacity. The equations for large deformations of circular plates of constant thickness  $h$  with axisymmetric boundary conditions can be found to be (based on formulae in [18, 19]),

$$\begin{aligned}\nabla_r^2 \nabla_r^2 w(r) &= \frac{h}{Dr} \left( \frac{d^2 w}{dr^2} \frac{d\Phi}{dr} + \frac{dw}{dr} \frac{d^2 \Phi}{dr^2} \right) + \frac{p_z(r)}{D}, \\ \nabla_r^2 \nabla_r^2 \Phi(r) &= -\frac{E}{r} \frac{dw}{dr} \frac{d^2 w}{dr^2},\end{aligned}\tag{21}$$

where  $\Phi$  is an Airy type stress function. These equations are a special form of von Kármán's equations, first derived by him in 1910. As well as boundary conditions on  $w$  as previously defined, we require boundary conditions on  $\Phi$ . At the moment, we are unsure of the proper approach to the boundary conditions for  $\Phi$ . The condition of no applied force on the outer boundary leads to  $\Phi''(r_0) = 0$ , and as for the small deformation case two constants are set to zero for a smooth solution at  $r = 0$ . One colleague suggested that the other condition at the outer edge should be  $\Phi'(r_0) = 0$ . However, another colleague and Miersemann & Mittelmann [10] suggested the conditions should be  $\Phi(r_0) = \Phi'(r_0) = 0$ . Obviously, further investigation of the literature is required to come up with a proper formulation. One possibility is Panc [12], which discusses refined plate theories where both bending and transverse shear effects are taken into account.

There are a number of ways of approaching the solution of (21) suggested in the literature. Since there are very few analytic solutions available, variational, finite element, finite element and integration techniques are suggested, within an iterative framework. One could start with  $\Phi_1 = 0$ , and solve the first equation in (21) for  $w_1$ , then substitute in the second equation in (21) and solve for  $\Phi_2$ , which can then be substituted into the first equation in (21) to solve for  $w_2$  and so on. This fixed point iterative approach generally converges. However, we would suggest that the solution of (21) with appropriate boundary conditions can be more easily approached as simply viewing it as a system of 8 first order nonlinear ode's, and solving using a simple shooting method.

### 5.3.2 Plates with Varying Thickness

If the flexural rigidity  $D$  is allowed to vary, then the formulation for the deformation of a plate becomes more complicated. This is equivalent to a plate with varying thickness, since  $D = Eh^3/12(1 - \nu^2)$ , and we usually assume the ma-

terial parameters  $E$  and  $\mu$  do not change throughout the material. The partial differential equation for the deformation becomes

$$\nabla^2 (D\nabla^2) - (1 - \nu) \left( \frac{\partial^2 D}{\partial x^2} \frac{\partial^2 w}{\partial y^2} - 2 \frac{\partial^2 D}{\partial x \partial y} \frac{\partial^2 w}{\partial x \partial y} + \frac{\partial^2 D}{\partial y^2} \frac{\partial^2 w}{\partial x^2} \right) = p_z. \quad (22)$$

In the situation of a circular plate with axisymmetric loading and where  $h$  and hence  $D$  are (known) functions of  $r$  only, this can be reduced to the (linear) ode

$$\nabla_r^2 (D\nabla_r^2 w(r)) - \frac{(1 - \nu)}{r} \left( \frac{d^2 w}{dr^2} \frac{dD}{dr} + \frac{dw}{dr} \frac{d^2 D}{dr^2} \right) = p_z. \quad (23)$$

While it is extremely unlikely that this fourth order ode could be solved analytically, a numerical solver for linear odes could be used to solve this quite simply.

### 5.3.3 Shallow Shells

The differential equations for the deformation of shallow shells with constant thickness are

$$\begin{aligned} D\nabla^2 \nabla^2 w &= hk_x \frac{\partial^2 \Phi}{\partial y^2} + hk_y \frac{\partial^2 \Phi}{\partial x^2} + p_z, \\ \frac{1}{E} \nabla^2 \nabla^2 \Phi &= -k_x \frac{\partial^2 w}{\partial y^2} - k_y \frac{\partial^2 w}{\partial x^2}, \end{aligned} \quad (24)$$

where  $k_x$  and  $k_y$  are the curvature in the  $x$  and  $y$  directions respectively, and  $\Phi$  is Airy's type of stress function. In the case that we are dealing with, a spherical cap,  $k_x = k_y = 1/R$  with  $R$  a constant, and after some derivation the deformation is the solution of

$$D\nabla^2 \nabla^2 w + \frac{Eh}{R^2} w = p_z. \quad (25)$$

Again assuming  $p_z$  and the boundary conditions are axisymmetric, we can reduce this to an ode. More information on the derivation of the equations for shells (not just shallow ones) can be found in, for example, Tomshenko & Woinowsky-Krieger [19], or Møllman [11].

## 6 Fracture Mechanics

While there was no time during the MISG study group to address the issues of when the lens will crack, and how the cracks will propagate, a large amount of work has been done in this area, and we would like to include a few comments on the literature that we have found. A full solution to the problem would require an application of these ideas to the lens problem.

Fracture mechanics is the theory behind why structures fail, usually through the propagation of cracks through the material. This is a relatively young field, with a variety of aspects, many of which are well summarised by Anderson [1] – an engineering text which considers both theoretical and practical aspects of fracture. Based upon the stress applied to a body, one can calculate when it will break due to cracks propagating through it. Whether or not the body already has flaws inherent in its structure when the stress is applied is also an important consideration. In the case of a coated lens, fracture could be caused by the stress of impact in a number of ways. The stress may not be sufficiently large to cause the uncoated lens to fracture. However, the usually more brittle thin coating on the back of the lens may fracture under the same stress. This then provides a local point on the main body of the lens where the stresses are much higher due to the fracture of the coating. The stress at this point may or may not be large enough to cause a complete failure of the lens, depending on the stresses involved and the strength of the lens material.

Another collection of texts that could be of use in solving this problem are edited by Sih [13, 14, 15, 16]. These are part of a larger collection of works on the mechanics of fracture, from a more mathematical point of view. Volume 1 [13] looks at a variety of methods for analysing mostly two-dimensional crack problems, concentrating on finding stress-intensity factors in various situations. One section particularly considers surface cracks, and another on integral transform methods looks at the stress near a star shaped crack. This is of particular interest here, since the crack structure of a lens after impact is star shaped. However, this section does not consider why star shaped cracks occur. Interestingly, Szilard [18] includes a section on yield-line analysis of plates, and includes a yield line patterns for various configurations that imply a star shaped fracture. Volume 2 [14] looks at three dimensional crack problems, and includes potentially useful contributions on cracks in structures made from bonding together two dissimilar materials (like a lens and its coating). Volume 3 [15] is devoted entirely to cracks in plates and shells. It includes sections on cracks through multilayered plates, cracks in spherical shells, and the dynamic analysis of cracked plates. Volume 7 [16] discusses experimental techniques for determining the important parameters in fracture mechanics.

## 7 Conclusion

During the initial presentation of the problem by SOLA, a “wishlist” was presented which outlined the company’s needs in this problem. The points, and what we accomplished were:

- *Develop a prediction of deflection on impact, based on lens form and material properties, including non-rotationally symmetrical forms.* We have looked at the equivalence of the dynamic and static tests, and identified

references that discuss how the forces due to impact can be modelled. The deflection of the lens can be modelled using thin plate and shell theory, although currently available theory does not allow for the solution of the completely general problem of interest to SOLA. While not discussed here, Szilard [18] includes an analytic solution for a simply supported circular plate with an off center point load, which will be of use.

- *Model the deformation and stresses in the back coatings of lenses under flexure.* The deformation of the back coatings will essentially be those of the lens itself. The work on cylindrical layers of dissimilar material under a moment gives us an idea on how the stress in the coatings is related to that in the lens itself.
- *Model the local stresses in the lens during flexure.* Thin plate and shell theory allows us to calculate stresses within the lens based upon the deformations, which in the case of circular geometries are the solutions to fourth order ordinary differential equations.
- *Model crack initiation and propagation.* While no work was directly done in this area, we have found several references that deal with closely related problems, particularly Anderson [1] and Sih [15].
- *Form a total predictive model for the lens/coating system at impact.* A full model would require many aspects, which we will consider below.

During the MISG some progress towards addressing the problem of lens fracture has been made. However, clearly much work remains to be done.

## 8 Acknowledgements

The project moderators, Jim Hill and Stephen Lucas, were greatly assisted by Philip Stephenson, Matthew Cuthbertson, David Lewis and Chong Kok from SOLA International, by their willingness to answer almost continual questions on the processes we were studying. We would also like to acknowledge the contributions from Alex Antic, Jamie Chamberlain, Dave Clements, Grant Cox, Kathrine Grillett, Miriam Hochwald, Phil Howlett, John King, Sean McElwain, Anna Milan, Julia Piantadosi, Colin Please, Boris Poliak, Don Vicendese, and Simon Watt.

## References

- [1] T.L. Anderson, *Fracture mechanics, fundamentals and applications, 2nd edition*, CRC Press, Boca Raton, 1995.

- [2] J.R. Barber, *Elasticity*, Kluwer Academic Publishers, , Dordrecht, 1993.
- [3] C.A. Brebbia, J.C.F. Telles & L.C. Wrobel, *Boundary element techniques, theory and applications in engineering*, Springer-Verlag, Berlin, 1984.
- [4] F. Essenburg, On surface constraints in plate problems, *J. Appl. Mech.*, **29** pp340–344, 1962.
- [5] G.M.L. Gladwell, *Contact problems in the classical theory of elasticity*, Sijthoff & Noordhoff, Alphen aan den Rijn, 1980.
- [6] W. Goldsmith *Impact, the theory and physical behaviour of colliding solids*, Edward Arnold (Publishers) Ltd., London, 1960.
- [7] K.L. Johnson, *Contact mechanics*, Cambridge University Press, Cambridge, 1985.
- [8] N. Kikuchi, *Finite element methods in mechanics*, Cambridge University Press, Cambridge, 1986.
- [9] L.D. Landau & E.M. Lifshitz, *Theory of elasticity, 3rd edition*, Pergamon Press, Oxford, 1986.
- [10] E. Miersemann & H.D. Mittelmann, Stability in obstacle problems for the von Karman plate, *SIAM J. Math. Anal.*, **23**, pp1099–1116, 1992.
- [11] H. Møllman, *Introduction to the theory of thin shells*, John Wiley & Sons, Chichester, 1981.
- [12] V. Panc, *Theories of elastic plates*, Noordhoff International Publishing, Leyden, 1975.
- [13] G.C. Sih (ed), *Mechanics of fracture 1, methods of analysis and solutions of crack problems*, Noordhoff International Publishing, Leyden, 1973.
- [14] G.C. Sih (ed), *Mechanics of fracture 2, three-dimensional crack problems*, Noordhoff International Publishing, Leyden, 1975.
- [15] G.C. Sih (ed), *Mechanics of fracture 3, plates and shells with cracks*, Noordhoff International Publishing, Leyden, 1977.
- [16] G.C. Sih (ed), *Mechanics of fracture 7, experimental evaluation of stress concentration and intensity factors*, Martinus Nijhoff Publishers, The Hague, 1981.
- [17] P. Stephenson, SOLA summary sheets for MISG 2000 meeting, 2000.
- [18] R. Szilard, *Theory and analysis of plates: classical and numerical methods*, Prentice-Hall, New Jersey, 1974.
- [19] S.P. Timoshenko & S. Woinowsky-Krieger, *Theory of plates and shells*, McGraw-Hill Book Company Inc., New York, 1959.

- [20] S.P. Timoshenko & J.N. Goodier, *Theory of elasticity, 3rd edition*, McGraw-Hill Book Company, New York, 1970.
- [21] D.R. Westbrook, The obstacle problem for beams and plates, *J. Comp. Appl. Math.*, **30** pp295–311, 1990.
- [22] S.T. Yau & Y. Gao, Obstacle problem for von Kármán equations, *Adv. Appl. Math.*, **13**, pp123–141, 1992.
- [23] Z.H. Zhong, *Finite element procedures for contact-impact problems*, Oxford University Press, Oxford, 1993.